8084 *Inorg. Chem.* **2009**, *48*, 8084–8091
DOI: 10.1021/ic900421v

Inorganic Chemistry
Article

Photochromic Ruthenium Sulfoxide Complexes: Evidence for Isomerization Through a Conical Intersection

Beth Anne McClure,[†] Nicholas V. Mockus,[†] Dennis P. Butcher, Jr.,[†] Daniel A. Lutterman,[†,‡] Claudia Turro,*[,†,‡] Jeffrey L. Petersen,[†,§] and Jeffrey J. Rack*[,†]

[†]*Department of Chemistry and Biochemistry, Ohio University, Athens, Ohio 45701,* [‡]*Department of Chemistry, The Ohio State University, Columbus, Ohio 43210, and* [§]*C. Eugene Bennett Department of Chemistry, West Virginia University, Morgantown, West Virginia 26506-6045*

Received March 4, 2009

The complexes $[Ru(bpy)_2(OS)](PF_6)$ and $[Ru(bpy)_2(OSO)](PF_6)$, where bpy is 2,2′-bipyridine, OS is 2-methylthiobenzoate, and OSO is 2-methylsulfinylbenzoate, have been studied. The electrochemical and photochemical reactivity of $[Ru(bpy)_2(OSO)]^+$ is consistent with an isomerization of the bound sulfoxide from S-bonded (*S*-) to O-bonded (*O*-) following irradiation or electrochemical oxidation. Charge transfer excitation of $[Ru(bpy)_2(OSO)]^+$ in MeOH results in the appearance of two new metal-to-ligand charge transfer (MLCT) maxima at 355 and 496 nm, while the peak at 396 nm diminishes in intensity. The isomerization is reversible at room temperature in alcohol or propylene carbonate solution. In the absence of light, solutions of *O*-$[Ru(bpy)_2(OSO)]^+$ revert to *S*-$[Ru(bpy)_2(OSO)]^+$. Kinetic analysis reveals a biexponential decay with rate constants of $5.66(3) \times 10^{-4}\ s^{-1}$ and $3.1(1) \times 10^{-5}\ s^{-1}$. Cyclic voltammograms of *S*-$[Ru(bpy)_2(OSO)]^+$ are consistent with electron-transfer-triggered isomerization of the sulfoxide. Analysis of these voltammograms reveal $E_S^{o\prime}$ = 0.86 V and $E_O^{o\prime}$ = 0.49 V versus Ag/Ag^+ for the S- and O-bonded $Ru^{3+/2+}$ couples, respectively, in propylene carbonate. We found $k_{S\rightarrow O}$ = 0.090(15) s^{-1} in propylene carbonate and $k_{S\rightarrow O}$ = 0.11(3) s^{-1} in acetonitrile on Ru^{III}, which is considerably slower than has been reported for other sulfoxide isomerizations on ruthenium polypyridyl complexes following oxidation. The photoisomerization quantum yield ($\Phi_{S\rightarrow O}$ = 0.45, methanol) is quite large, indicating a rapid excited state isomerization rate constant. The kinetic trace at 500 nm is monoexponential with τ = 150 ps, which is assigned to the excited S→O isomerization rate. There is no spectroscopic or kinetic evidence for an O-bonded ^{3}MLCT excited state in the spectral evolution of *S*-$[Ru(bpy)_2(OSO)]^+$ to *O*-$[Ru(bpy)_2(OSO)]^+$. Thus, isomerization occurs nonadiabatically from an S-bonded (or η^2-sulfoxide) ^{3}MLCT excited state to an O-bonded ground state. Density functional theory calculations support the assigned spectroscopy and provide insight into ruthenium ligand bonding.

Introduction

In 1970, Forster classified photochemical reactions as either adiabatic or nonadiabatic, depending upon whether the chemical reaction occurred on a potential energy surface of identical multiplicity or one of different multiplicity.[1] These concepts have since been expanded to focus not solely on spin, such that adiabatic reactions are those that separate atomic and electronic movement (Born−Oppenheimer approximation), while nonadiabatic reactions are those that involve nuclear dynamics on two separate potential energy curves.[2,3] The latter may indeed be much more common than originally thought. In mapping potential energy surfaces, recent computational studies have revealed conical intersections at which the excited-state molecule may rapidly undergo nonradiative decay to the ground-state potential energy surface.[4−6] Such regions occur at the intersection of two or more orthogonal reaction coordinates in the evolution of an excited state. These pathways provide a facile mechanism for the formation of a photoproduct with little to no activation barrier. This issue is especially important in photochemical isomerizations where substantial changes in atomic connectivity and electronic structure occur on a femtosecond or picosecond time scale. Efficient conversion of photonic energy to potential energy in these reactions requires minimal energy pathways for the formation of photoproducts.

*To whom correspondence should be addressed. E-mail: rackj@ohio.edu (J.J.R.).

(1) Forster, T. *Pure Appl. Chem.* **1970**, *24*, 443–449.
(2) Domcke, W.; Yarkony, D. R.; Koppel, H. *Conical Intersections: Electronic Structure, Dynamics and Spectroscopy*; World Scientific: River Edge, NJ, **2004**.
(3) Worth, G. A.; Cederbaum, L. S. *Annu. Rev. Phys. Chem.* **2004**, *55*, 127–158.
(4) Dick, B.; Haas, Y.; Zilberg, S. *Chem. Phys.* **2008**, *347*, 65–77.
(5) Piryatinski, A.; Tretiak, S.; Chernyak, V. Y. *Chem. Phys.* **2008**, *347*, 25–38.
(6) Quenneville, J.; Martinez, T. J. *J. Phys. Chem. A* **2003**, *107*, 829–837.

 Published on Web 05/12/2009

Photochromic molecules are a special case of photochemical isomerization.[7−11] The resultant photochemical product, or metastable state, exhibits a substantially different atomic and electronic structure than the initial ground state. Mechanistic studies that reveal the nature of coupling between atomic structure and electronic state relaxation in these complexes are of fundamental importance. For example, photochromic molecules have featured prominently in the construction of logic gates,[12−14] photoswitches,[15−19] and other photoresponsive materials.[20−26] For our part, we have developed a class of synchronously photochromic and electrochromic ruthenium and osmium polypyridine sulfoxide compounds that operate at room temperature, in the solid state, and switch on the picosecond to nanosecond time scale.[27−36] The photochromic action is due to a photo-triggered isomerization of the bound sulfoxide from S- to O-bonded. Reversion of the metastable O-bonded product to the S-bonded starting material occurs either photochemically or thermally, depending upon the nature of the metal atom and the ancillary ligands. In our studies of $[Ru(bpy)_2(OSO)]^+$,[37] where bpy is 2,2′-bipyridine and OSO is 2-methylsulfinylbenzoate, we have found evidence for a nonadiabatic isomerization on the picosecond time scale from S- to O-bonded sulfoxide.

Experimental Section

The compound *cis*-$Ru(bpy)_2Cl_2 \cdot xH_2O$ was either synthesized using published methods[38] or purchased from Strem and used as received. The reagents bpy, 2-(methylthio)benzoic acid (OS), and 3-chloroperbenzoic acid (*m*-cpba) were purchased from Aldrich and used as received. Solvents such as methanol (MeOH), ethanol (EtOH), anhydrous propylene carbonate, 1,2-dichloroethane, and diethyl ether (Et_2O) were purchased from Aldrich and used without further purification. Acetonitrile for electrochemical measurements was HPLC-grade purchased from Burdick and Jackson and used without further purification. Tetrabutylammonium hexafluorophosphate ($TBAPF_6$) was purchased from Aldrich and recrystallized three times from ethanol before use.

$[Ru(bpy)_2(OS)](PF_6)$. Dark purple *cis*-$Ru(bpy)_2Cl_2$ (200 mg, 0.384 mmol), OS (71.1 mg, 0.422 mmol), 120 μL of triethylamine, and 2 equiv of $AgPF_6$ (194 mg, 0.768 mmol) were dissolved in 125 mL of 1,2-dichloroethane. The reaction was refluxed for 4 h under argon. The solution changed from purple to deep red as the reaction progressed, during which time solid AgCl precipitated. The solution was cooled to −30 °C overnight to ensure full precipitation of AgCl and then filtered to collect 2 equiv of AgCl. The filtrate was subsequently removed by rotary evaporation. The resulting solid was dissolved in 25 mL of dichloromethane and extracted with a 10 mL of an aqueous solution of 30 mg of $LiOH \cdot H_2O$ to remove NEt_3HPF_6 formed during reaction. The dichloromethane layer was dried with magnesium sulfate, and the solvent was removed by rotary evaporation. The solid was dissolved in about 5 mL of ethanol. Ether was added to precipitate a red solid. The product was isolated via vacuum filtration, washed with ether (3 × 15 mL), and air-dried. Yield: 210 mg (75%). UV−vis (MeOH): λ_{max} = 467 nm (5510 $M^{-1}cm^{-1}$). $E^{o\prime}$ $Ru^{3+/2+}$ vs Ag/AgCl = 1.0 V. ^1H NMR (CD_3CN, 300 MHz): δ 9.15 (d, bpy, 1 H), 8.84 (d, bpy, 1 H), 8.67 (d, bpy, 1 H), 8.53 (d, 3 H), 8.27 (t, bpy, 1 H), 8.00 (m, 3 H), 7.90 (t, bpy, 1 H), 7.80 (m, 2 H), 7.70 (d, S−O, 1 H), 7.50 (m, 3 H), 7.33 (m, 2 H), 7.28 (t, bpy, 1 H), 1.86(s, SCH_3, 3 H). Elem anal. calcd for $[Ru(C_{10}H_8N_2)_2(C_8H_7O_2S)]PF_6 \cdot H_2O \cdot 0.2Et_2O$: C, 45.64%; H, 3.60%; O, 6.76%; N, 7.39%; S, 4.23%. Found: C, 45.79%; H, 3.50%; O, 6.54%; N, 7.46%; S, 4.11%.

$[Ru(bpy)_2(OSO)](PF_6)$. Red $[Ru(bpy)_2(OS)](PF_6)$ (50.00 mg, 0.0689 mmol) and *m*-CPBA (26.16 mg, 0.1516 mmol) were dissolved in 50 mL of methanol. The reaction was stirred at room temperature in the dark for 4 h. The progress of the reaction was monitored by the ^{3}MLCT transition via UV−vis spectroscopy (MLCT = metal-to-ligand charge transfer). The solution volume was reduced to < 5 mL and the product precipitated through the addition of ether. The yellow-orange product was isolated by vacuum filtration. Excess *m*-CPBA and the reduced product, 3-chlorobenzoic acid, were removed by washing the solid ruthenium product with ether (3 × 15 mL) and air-dried. Yield: 41.5 mg (83%). UV−vis (MeOH): λ_{max} = 396 nm (S-bonded) (6710 $M^{-1}cm^{-1}$). $E^{o\prime}$ $Ru^{3+/2+}$ vs Ag/Ag^+ = 0.90 V (S-bonded), 0.54 V (O-bonded). Emission (4:1 EtOH/MeOH, 77 K): λ_{max} = 580 nm, Φ = 0.042

(7) Irie, M. *Chem. Rev.* **2000**, *100*, 1685–1716.
(8) Kume, S.; Nishihara, H. *Dalton Trans.* **2008**, 3260–3271.
(9) To, T. T.; Duke, C. B.; Junker, C. S.; O'Brien, C. M.; Ross, C. R.; Barnes, C. E.; Webster, C. E.; Burkey, T. J. *Organometallics* **2008**, *27*, 289–296.
(10) To, T. T.; Heilweil, E. J.; Duke, C. B.; Burkey, T. J. *J. Phys. Chem. A* **2007**, *111*, 6933–6937.
(11) Finden, J.; Kunz, T. K.; Branda, N. R.; Wolf, M. O. *Adv. Mater.* **2008**, *20*, 1998–2002.
(12) Andreasson, J.; Straight, S. D.; Bandyopadhyay, S.; Mitchell, R.; Moore, T. A.; Moore, A. L.; Gust, D. *Angew. Chem., Int. Ed.* **2007**, *46*, 958–961.
(13) Andreasson, J.; Straight, S. D.; Moore, T. A.; Moore, A. L.; Gust, D. *J. Am. Chem. Soc.* **2008**, *130*, 11122–11128.
(14) Straight, S. D.; Liddell, P. A.; Terazono, Y.; Moore, T. A.; Moore, A. L.; Gust, D. *Adv. Funct. Mater.* **2007**, *17*, 777–785.
(15) Belser, P.; De Cola, L.; Hartl, F.; Adamo, V.; Bozic, B.; Chriqui, Y.; Iyer, V. M.; Jukes, R. T. F.; Kuhni, J.; Querol, M.; Roma, S.; Salluce, N. *Adv. Funct. Mater.* **2006**, *16*, 195–208.
(16) Bonnet, S.; Collin, J.-P.; Sauvage, J.-P. *Inorg. Chem.* **2006**, *45*, 4024–4034.
(17) Sato, O. *Acc. Chem. Res.* **2003**, *36*, 692–700.
(18) Raymo, F. M.; Tomasulo, M. *Chem.—Eur. J.* **2006**, *12*, 3186–3193.
(19) Tomasulo, M.; Deniz, E.; Alvarado, R. J.; Raymo, F. M. *J. Phys. Chem. C* **2008**, *112*, 8038–8045.
(20) Ikeda, T.; Nakano, M.; Yu, Y.; Tsutsumi, O.; Kanazawa, A. *Adv. Mater.* **2003**, *15*, 201–205.
(21) Yu, Y.; Nakano, M.; Ikeda, T. *Nature* **2003**, *425*, 145–145.
(22) Fally, M.; Imlau, M.; Rupp, R. A.; Ellabban, M. A.; Woike, T. *Phys. Rev. Lett.* **2004**, *93*, 243903.
(23) Gutlich, P.; Garcia, Y.; Woike, T. *Coord. Chem. Rev.* **2001**, *219−221*, 839–879.
(24) Imlau, M.; Fally, M.; Weisemoeller, T.; Schaniel, D.; Herth, P.; Woike, T. *Phys. Rev. B* **2006**, *73*, 205113.
(25) Schaniel, D.; Imlau, M.; Weisemoeller, T.; Woike, T.; Kramer, K. W.; Gudel, H.-U. *Adv. Mater.* **2007**, *19*, 723–726.
(26) Kobatake, S.; Takami, S.; Muto, H.; Ishikawa, T.; Irie, M. *Nature* **2007**, *446*, 778–781.
(27) Mockus, N. V.; Marquard, S.; Rack, J. J. *J. Photochem. Photobiol. A* **2008**, *200*, 39–43.
(28) Mockus, N. V.; Petersen, J. L.; Rack, J. J. *Inorg. Chem.* **2006**, *45*, 8–10.
(29) Mockus, N. V.; Rabinovich, D.; Petersen, J. L.; Rack, J. J. *Angew. Chem., Int. Ed.* **2008**, *47*, 1458–1461.
(30) Rachford, A. A.; Petersen, J. L.; Rack, J. J. *Inorg. Chem.* **2005**, *44*, 8065–8075.
(31) Rachford, A. A.; Petersen, J. L.; Rack, J. J. *Inorg. Chem.* **2006**, *45*, 5953–5960.
(32) Rachford, A. A.; Petersen, J. L.; Rack, J. J. *Dalton Trans.* **2007**, 3245–3251.
(33) Rachford, A. A.; Rack, J. J. *J. Am. Chem. Soc.* **2006**, *128*, 14318–14324.
(34) Rack, J. J.; Mockus, N. V. *Inorg. Chem.* **2003**, *42*, 5792–5794.
(35) Rack, J. J.; Rachford, A. A.; Shelker, A. M. *Inorg. Chem.* **2003**, *42*, 7357–7359.
(36) Rack, J. J.; Winkler, J. R.; Gray, H. B. *J. Am. Chem. Soc.* **2001**, *123*, 2432–2433.
(37) Butcher, D. P.Jr.; Rachford, A. A.; Petersen, J. L.; Rack, J. J. *Inorg. Chem.* **2006**, *45*, 9178–9180.
(38) Sullivan, B. P.; Salman, D. J.; Meyer, T. J. *Inorg. Chem.* **1978**, *17*, 3334–3341.

(S-bonded, λ_{exc} = 400 nm). ^{1}H NMR (CD_3OD, 500 MHz): δ 9.18 (d, bpy, 1 H), 8.93 (d, bpy, 1 H), 8.83 (d, bpy, 1 H), 8.62 (d, bpy, 1 H), 8.61 (d, bpy, 1 H), 8.57 (d, bpy, 1 H), 8.47 (t, bpy, 1 H), 8.33 (d, OS-O, 1 H), 8.16 (t, bpy, 1 H), 8.06 (t, bpy, 1 H), 8.05 (t, bpy, 1 H), 8.01 (t, bpy, 1 H), 7.97 (d, OS-O, 1 H), 7.93 (d, bpy, 1 H), 7.90 (t, OS-O, 1 H), 7.67 (t, OS-O, 1 H), 7.60 (d, bpy, 1 H), 7.51 (t, bpy, 1 H), 7.38 (t, bpy, 1 H), 7.35 (t, bpy, 1 H), 2.76 (s, $OSCH_3$, 3H). Elem anal. calcd for $[Ru(C_{10}H_8N_2)_2(C_8H_7O_3S)]PF_6 \cdot H_2O \cdot 0.2Et_2O$: C, 44.66%; H, 3.52%; O, 8.68%; N, 7.24%; S, 4.14%. Found: C, 44.45%; H, 3.15%; O, 8.95%; N, 7.16%; S, 3.87%.

2-Methanesulfinyl-benzoic acid. In 30 mL of chloroform, OS (57 mg, 0.339 mmol) was dissolved. In a separate 30 mL of chloroform, 3-chloroperoxybenzoic acid (99 mg 60% peroxo reagent by ^{1}H NMR, 0.339 mmol) was dissolved and added slowly to the OS solution. The combined solution was stirred at room temperature for 10 min. The solvent was removed by rotary evaporation. The resulting solid was rinsed from the flask with 2 mL of diethyl ether and isolated by vacuum filtration. The solid was rinsed with an additional 5 mL of diethyl ether and air-dried. Yield: 33 mg (53%). ^{1}H NMR ($CDCl_3$, 300 MHz): δ 8.33 (d, 1H), 8.18 (d, 1H), 7.86 (t, 1H), 7.61 (d, 1H), 2.92 (s, 3H). Elem anal. calcd for $C_8H_7O_3S$: C, 52.34%; H, 4.37%; O, 25.94%; S, 17.33%. Found: C, 51.98%; H, 4.39%; O, 26.10%; S, 17.14%.

$[Ru(bpy)_2(OSO)](PF_6)$ Alternative Synthesis. In a procedure similar to that described for $[Ru(bpy)_2(OS)](PF_6)$, *cis*-$[Ru(bpy)_2Cl_2]$ (110 mg, 0.211 mmol), OSO (45 mg, 0.242 mmol), triethylamine (150 μL), and 2 equiv of $AgPF_6$ (109 mg, 0.429 mmol) were dissolved in 40 mL of ethanol in the dark or under red light. The reaction mixture was refluxed under nitrogen for 4 h. The solution was cooled overnight at −30 °C and isolated under red light following the same procedure as for $[Ru(bpy)_2(OS)](PF_6)$ described above. Yield: 97 mg (62%). Characterization of the product agrees with that obtained by the above procedure.

Cyclic voltammetry was performed on a CH Instruments CHI 730A electrochemical analyzer. This workstation contains a digital simulation package as part of the software package to operate the workstation (CHI, version 2.06). The working electrode was either a Pt or glassy carbon disk (Cypress Systems) electrode where the electrode surface is 1.0 mm for Pt or 1.5 mm for glassy carbon[2]. The counter and reference electrodes were Pt wire and Ag/Ag^+, respectively. Electrochemical measurements were performed in acetonitrile or propylene carbonate solutions containing 0.1 M $TBAPF_6$ electrolyte in a one compartment cell. Cyclic voltammagrams were collected at various scan rates over the range of 0.01−5.0 V s^{-1}. To determine the rate of electrochemically induced isomerization, the ratios of cathodic peak current $(i_c)_o$ and anodic peak current $(i_a)_o$ of the S-bonded peak were plotted as a function of time, τ, following a previously described method.[39] However, unlike the system described by Rocha, isomerization succeeds oxidation rather than reduction of the metal complex, and therefore the ratio $(i_c)_o/(i_a)_o$ is plotted as a function of time instead of $(i_a)_o/(i_c)_o$. The time was determined as 2 times the difference between the switching potential and $E^{o\prime}$ divided by the scan rate. The plots of $(i_c)_o/(i_a)_o$ versus τ were fit to first-order exponential decay curves to yield the rate constant of S to O isomerization of the Ru^{3+} species.

Electronic absorption spectra were collected on an Agilent 8453 spectrophotometer. Kinetic analyses of O→S rates determined in solution were performed on this same spectrometer. Bulk photolysis experiments were conducted using a 75 or 100 W xenon-arc lamp (Oriel) fitted with a Canon standard camera UV filter.

Picosecond transient absorption spectra were acquired at the Ohio Laboratory for Kinetic Spectrometry (OLKS) as part of Bowling Green State University's (BGSU) Center for Photochemical Studies. The experimental details were described previously, and only a brief discussion is provided here.[40−42] Spectra-Physics Hurricane Evolution and Ti:sapphire were combined to yield 800 nm pulses of 130 fs in duration at a rate of 1 kHz. The excitation wavelength of 400 nm (~2 μJ/pulse) was obtained from frequency-doubling the Ti:Sapphire fundamental. A portion of the 800 nm fundamental was employed to generate the white-light continuum probe source by focusing the light through a CaF_2 plate. Detection from ~360 to 750 nm was achieved with a double CCD spectrograph. Transient spectra at a particular delay time represent the average of 4000 excitation pulses. The instrument is operated through an in-house (BGSU) LabVIEW software routine. Kinetic analysis of the data was performed at Ohio University (OU) with the SPECFIT (version 3.0.37, Spectrum Software Associates) program, a global analysis routine based on single-value decomposition. Goodness-of-fit was evaluated qualitatively by inspection of the residual plots. For the S-bonded complex, samples were prepared in bulk solution and analyzed using a flow-through cell with a flow rate of approximately 15 mL/s. For the O-bonded isomer, a steady-state cell containing a small portion of the same solution was used.

All calculations were performed using the Gaussian 03 program package,[43] with the Becke three-parameter hybrid exchange and the Lee−Yang−Parr correlation functionals (B3LYP).[44−46] The 6-31G* basis set was used for H, C, N, O, and S (using five pure d functions),[47] along with the Stuttgart/Dresden energy-consistent pseudopotentials for Ru.[48,49] All geometry optimizations were performed in C_1 symmetry with subsequent vibrational frequency analysis to confirm that each stationary point was a minimum on the potential energy surface. Solvent effects were modeled by single point calculations based on the gas-phase optimized structures using the polarizable continuum model.[50,51] Orbital analysis was computed using Molekel 4.3.win32.[52] Singlet vertical excitation energies were computed using the time-dependent density functional theory (TD-DFT) approach as implemented in Gaussian 03 using the basis sets described above.[53−55]

The percentage of atomic character in some of the occupied (canonical) molecular orbitals (MOs) in the complexes was calculated from a full population analysis, using eq 1

$$\text{percent character} = \frac{\sum \phi_i^2}{\sum \phi_{\text{all}}^2} \times 100\% \qquad (1)$$

(39) Rocha, R. C.; Toma, H. E. *Trans. Met. Chem.* **2003**, *28*, 43–50.

(40) Nikolaitchik, A. V.; Korth, O.; Rodgers, M. A. J. *J. Phys. Chem. A* **1999**, *103*, 7587–7596.

(41) Okhrimenko, A. N.; Gusev, A. V.; Rodgers, M. A. J. *J. Phys. Chem. A* **2005**, *109*, 7653–7656.

(42) Pelliccioli, A. P.; Henbest, K.; Kwag, G.; Carvagno, T. R.; Kenney, M. E.; Rodgers, M. A. J. *J. Phys. Chem. A* **2001**, *105*, 1757–1766.

(43) Frisch, M. J. et al. *Gaussian 03*, C.02 ed.; Gaussian Inc: Wallingford, CT, **2004**.

(44) Becke, A. D. *Phys. Rev. A* **1988**, *38*, 3098–3100.

(45) Becke, A. D. *J. Chem. Phys.* **1993**, *98*, 5648–5652.

(46) Lee, C. T.; Yang, W. T.; Parr, R. G. *Phys. Rev. B* **1988**, *37*, 785–789.

(47) Hehre, W. J.; Radom, L.; Schleyer, P. v. R.; Pople, J. A. *Ab Initio Molecular Orbital Theory*; John Wiley & Sons: New York, **1986**.

(48) Dolg, M.; Stoll, H.; Preuss, H. *Theor. Chim. Acta* **1993**, *85*, 441–450.

(49) Wedig, U.; Dolg, M.; Stoll, H. *Quantum Chemistry: The Challenge of Transition Metals and Coordination Chemistry*; Springer: Dordrecht, The Netherlands, **1986**.

(50) Cances, E.; Mennucci, B.; Tomasi, J. *J. Chem. Phys.* **1997**, *107*, 3032–3041.

(51) Tomasi, J.; Persico, M. *Chem. Rev.* **1994**, *94*, 2027–2094.

(52) Flukiger, P.; Luthi, H. P.; Portmann, S.; Weber, J. *Molekel 4.3.win32*; Swiss Center for Scientific Computing: Manno, Switzerland, **2000**.

(53) Bauernschmitt, R.; Ahlrichs, R. *Chem. Phys. Lett.* **1996**, *256*, 454–464.

(54) Casida, M. E.; Jamorski, C.; Casida, K. C.; Salahub, D. R. *J. Chem. Phys.* **1998**, *108*, 4439–4449.

(55) Stratmann, R. E.; Scuseria, G. E.; Frisch, M. J. *J. Chem. Phys.* **1988**, *109*, 8218–8224.

where $\sum \phi_i^2$ (i = Ru, O, N, or S) is the sum of the squares of the eigenvalues associated with the atomic orbital (AO) of one atom and $\sum \phi_{all}^2$ is the sum of the squares of the eigenvalues for all of the AOs in a particular MO. This calculation was performed on each of the three highest-occupied MOs.

Results and Discussion

We previously communicated the structural and basic spectroscopic and electrochemical properties of [Ru(bpy)$_2$(OS)](PF$_6$) and [Ru(bpy)$_2$(OSO)](PF$_6$).[37] Briefly, the reaction of 2-(methylthio)benzoic acid with Ru(bpy)$_2$Cl$_2$ in the presence of NEt$_3$ and 2 equiv of AgPF$_6$ affords [Ru(bpy)$_2$(OS)](PF$_6$) in good yield. The sulfoxide complex, [Ru(bpy)$_2$(OSO)](PF$_6$), was prepared by reaction of the ruthenium thioether complex with *m*-cpba in essentially quantitative yield. Alternatively, reaction of this sulfoxide, produced independently from 2-methylthiobenzoic acid and *m*-cpba, with Ru(bpy)$_2$Cl$_2$ and AgPF$_6$ yields [Ru(bpy)$_2$(OSO)](PF$_6$). The molecular structures of both cations are shown in Figure 1. Of note is a shortening of the Ru−S bond distance from 2.3328(8) to 2.2130(7) Å upon oxidation of the coordinated thioether to the coordinated sulfoxide. The trans Ru−N3 bond distance lengthens accordingly from 2.066(2) to 2.098(2) Å upon oxidation to form the coordinated sulfoxide. The S−O bond distance in the free sulfoxide (1.515(2) Å, Supporting Information) is longer than that observed in the bound sulfoxide complex (1.479(2) Å), indicating that the S=O bond is stronger in the complex than in the unbound ligand. These bond distances and changes indicate a strong bonding interaction between ruthenium and the sulfoxide.

The visible absorption spectra of [Ru(bpy)$_2$(OS)]$^+$ and [Ru(bpy)$_2$(OSO)]$^+$ are dominated by Ru dπ → bpy π^* MLCT transitions. This transition is found at 467 nm (ε = 5510 M^{-1} cm^{-1}) for the thioether complex, which shifts to 396 nm (ε = 6710 M^{-1} cm^{-1}) in the sulfoxide complex. The dramatic blue shift in this lowest-energy feature is indicative of significant ruthenium dπ stabilization afforded by the sulfoxide relative to the thioether. For comparison, [Ru(bpy)$_2$(pic)]$^+$, where pic is 2-pyridinecarboxylate, features a lowest-energy absorption maximum at 483 nm.[56] This example directly compares pyridine with sulfoxide in the inner coordination sphere and demonstrates the substantial ruthenium dπ stabilization by the sulfoxide. Additional absorption maxima for other relevant bis(bipyridine)ruthenium complexes are as follows: [Ru(bpy)$_2$(NCCH$_3$)$_2$]$^{2+}$ (426 nm), [Ru(bpy)$_2$(pyridine)$_2$]$^{2+}$ (456 nm), and [Ru(bpy)$_2$(CN)$_2$] (458 nm).[57] In aggregate, the relative absorption maximum (396 nm) and short Ru−S bond in [Ru(bpy)$_2$(OSO)]$^+$ are suggestive of significant mixing between ruthenium and sulfur.

In accord with these observations, [Ru(bpy)$_2$(CO)$_2$]$^{2+}$ displays a lowest-energy absorption maximum at 305 nm.[58] This maximum is dramatically blue-shifted relative to the complexes listed above. In addition, emission from this complex at 77 K is assigned to an intraligand bpy $\pi^* \rightarrow \pi$ transition with the first structured peak appearing near 400 nm. It is clearly distinct from the CT emission that is typically observed in ruthenium polypyridine complexes near 600 nm. The π^* orbitals of CO ligands must mix strongly with the Ru dπ set yielding mixed t$_{2g}$-type orbitals that contain significant Ru and CO character. Or, as the authors of this report state, the Ru dπ set is stabilized to an extent that they are now below the filled π MOs of bpy.

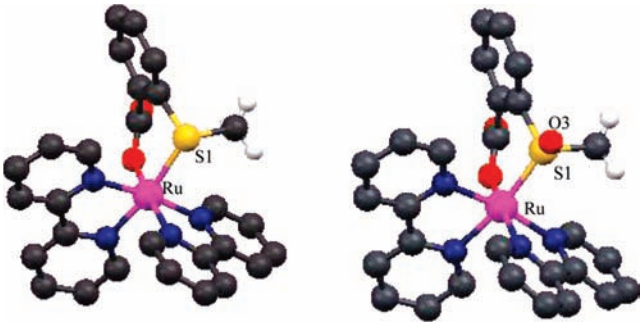

Figure 1. Structures of [Ru(bpy)$_2$(OS)]$^+$ and [Ru(bpy)$_2$(OSO)]$^+$ viewed down the pseudo-three-fold axis, where OS is 2-methylthiobenzoate and OSO is 2-methylsulfinylbenzoate. Certain hydrogen atoms are removed for clarity

Given the dramatic blue shift in the CT manifold for [Ru(bpy)$_2$(OSO)]$^+$ relative to [Ru(bpy)$_2$(OS)]$^+$ and other ruthenium polypyridine complexes, DFT calculations were performed to gain insight into the electronic nature of these complexes. These calculations predicted the three highest molecular orbitals for [Ru(bpy)$_2$(OS)]$^+$ to be in descending order d$_{xz}$, d$_{xy}$, and d$_{yz}$, with the *z* axis aligned along the Ru−S bond (Supporting Information). These MOs are separated by a total energy of 0.55 eV (4436 cm^{-1}). This separation is large in comparison to [Ru(bpy)$_2$(NCCH$_3$)$_2$]$^{2+}$ and [Ru(bpy)$_2$(CN)$_2$], where the corresponding separation in the Ru(dπ) manifold is 0.21 (1694 cm^{-1}) and 0.20 eV (1613 cm^{-1}), respectively. The d$_{xz}$ and d$_{xy}$ orbitals in [Ru(bpy)$_2$(OS)]$^+$ are positioned on the axis containing the Ru−O bond and are π^* with respect to the interaction between oxygen and nitrogen atoms. This antibonding contribution serves to destabilize these orbitals, leading to a larger separation than that found in [Ru(bpy)$_2$(NCCH$_3$)$_2$]$^{2+}$ and [Ru(bpy)$_2$(CN)$_2$]. The calculations also reveal a larger contribution of oxygen and sulfur character in these primarily Ru dπ orbtials. For example, in [Ru(bpy)$_2$(NCCH$_3$)$_2$]$^{2+}$ and [Ru(bpy)$_2$(CN)$_2$], the NCCH$_3$ nitrogen and CN$^-$ carbon contribute 0.2−0.3% and the nitrogens from the bpy ligand contribute on average 0.2−0.7% to the character of the Ru(dπ) MOs (Tables S1 and S2, Supporting Information). For [Ru(bpy)$_2$(OS)]$^+$, the oxygen contribution to d$_{xz}$ and d$_{xy}$ is 5.8 and 5.9%, respectively (Table S3, Supporting Information). The d$_{xz}$ is further destabilized by a π^* interaction with sulfur AOs, which contributes 4.4% to this MO. The d$_{yz}$ lies perpendicular to the Ru−O bond and therefore cannot interact with the oxygen atom; however, its orientation allows for interactions with the sulfur AOs, which account for 0.9% of the MO in a π-bonding or stabilizing manner. The significant mixing of π-stabilizing and π-destabilizing ligands results in a large separation of orbitals in the Ru(dπ) set.

When [Ru(bpy)$_2$(OS)]$^+$ is oxidized to [Ru(bpy)$_2$(OSO)]$^+$, the electron deficiency on sulfur creates a stronger bond to ruthenium. This is evidenced by a shortening of the Ru−S bond in the calculated structure of [Ru(bpy)$_2$(OS)]$^+$ from 2.40 to 2.29 Å in [Ru(bpy)$_2$(OSO)]$^+$, which matches well with the reported bond lengths from the crystal structure (see

(56) Norrby, T.; Borje, A.; Akermark, B.; Hammarstrom, L.; Alsins, J.; Lashgari, K.; Norrestam, R.; Martensson, J.; Stenhagen, G. *Inorg. Chem.* **1997**, *36*, 5850–5858.
(57) Juris, A.; Balzani, V.; Barigelletti, F.; Campagna, S.; Belser, P.; Von Zelewsky, A. *Coord. Chem. Rev.* **1988**, *84*, 85–277.
(58) Pinnick, D. V.; Durham, B. *Inorg. Chem.* **1984**, *23*, 1440–1445.

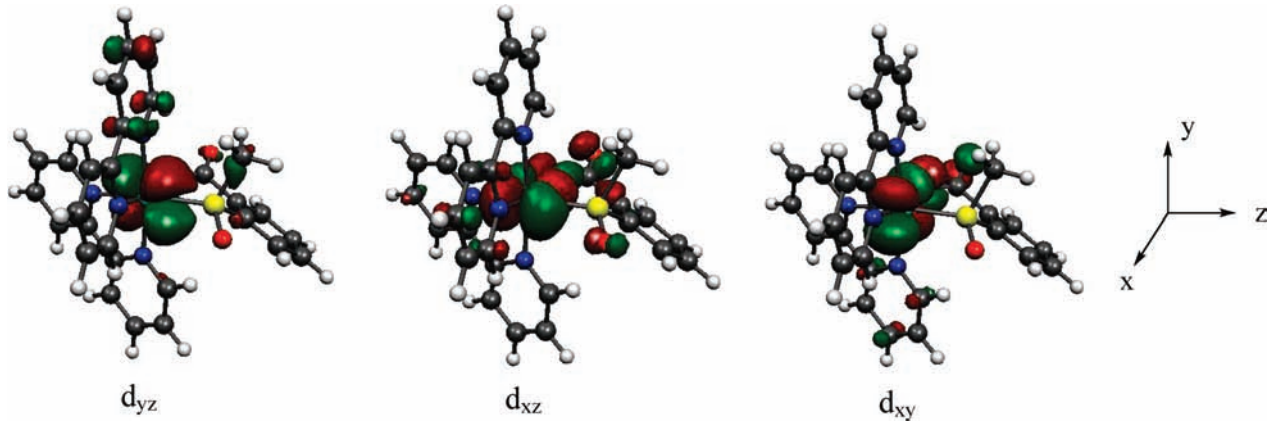

Figure 2. Highest-occupied Ru dπ orbital manifold obtained from DFT calculations for $[Ru(bpy)_2(OSO)]^+$.

above). The stronger bond between the ruthenium and sulfur atoms is also observed in the Ru(dπ) orbital manifold of $[Ru(bpy)_2(OSO)]^+$ (Figure 2), which features a dramatic rearrangement in the Ru(dπ) set, as compared to $[Ru(bpy)_2(OS)]^+$. While the energy of d_{xy} remains unaffected because it is perpendicular to the Ru−S bond, both d_{xz} and d_{yz} are stabilized due to the interaction with sulfur. This stabilization is due to a new π-bonding interaction with the sulfur, which contributes 1.3 and 1.8% to the MOs, respectively (Table S4, Supporting Information). By lowering these two MOs, the total energy span in the Ru(dπ) set increases to 0.65 eV (5243 cm^{-1}; relative to 0.55 eV above). It should be noted that, like $[Ru(bpy)_2(OS)]^+$, the d_{xy} and d_{xz} have large contributions (8.9 and 6.9%, respectively) in a π^* interaction from the bound carboxylate oxygen. The calculations demonstrate significant mixing of the Ru(dπ) set with the chelating sulfoxide ligand.

TD-DFT studies were employed to probe the nature of the lowest-energy transitions in these complexes. For $[Ru(bpy)_2(OS)]^+$, a transition with ^{1}MLCT character and assigned to Ru $d_{xz} \rightarrow$ bpy π^* is predicted at 470 nm (f = 0.0907). This corresponds remarkably well with the observed visible spectrum. Compared to $[Ru(bpy)_2(OS)]^+$, a dramatic blue shift is observed in the TD-DFT results of $[Ru(bpy)_2(OSO)]^+$, where two dominant low-energy transitions are predicted at 422 nm (f = 0.0625) and 379 nm (f = 0.0623) with ^{1}MLCT character, which are ascribed as Ru $d_{xz} \rightarrow$ bpy π^* and Ru $d_{yz} \rightarrow$ bpy π^*, respectively. The visible spectrum in solution reveals a single, broad band at 396 nm that likely contains these two transitions. In accord with the structural and absorption data, it appears from these results that MLCT excitation occurs from an orbital containing significant ruthenium and sulfoxide character to an orbital localized on bipyridine. Oxidation of this orbital either through photochemical or electrochemical action will result in substantial weakening of the Ru−S bond.

Charge transfer excitation of $[Ru(bpy)_2(OSO)]^+$ in MeOH results in the appearance of two new MLCT maxima at 355 and 496 nm, while the peak at 396 nm diminishes in intensity (Figure 3). This change in absorption maxima is consistent with an O-bonded sulfoxide in accord with previous results

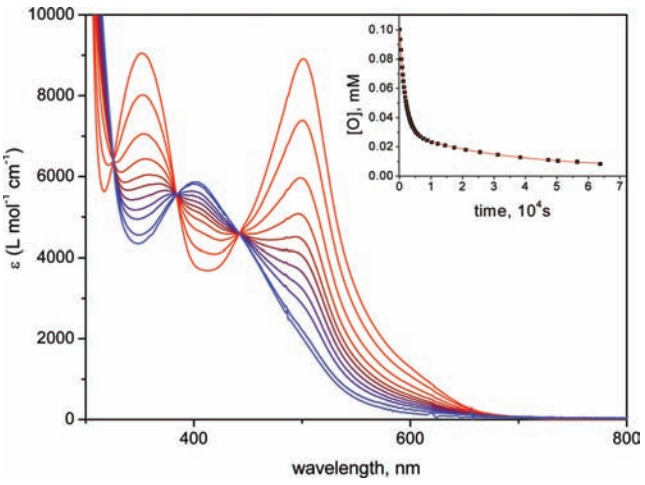

Figure 3. UV−visible spectra of *S*- (blue) and *O*-$[Ru(bpy)_2(OSO)]^+$ (red) and thermal reversion spectral traces from O-bonded to S-bonded. Inset: plot of concentration of *O*-$[Ru(bpy)_2(OSO)]^+$ versus time, clearly indicating biexponential behavior.

on sulfoxide isomerization.[59−61] Moreover, these new maxima are in agreement with other spectra containing the $[Ru(bpy)_2]^{2+}$ fragment with two O-bonded ligands. For example, $[Ru(bpy)_2(OH_2)_2]^{2+}$ (λ_{max} = 355, 498 nm; aqueous solution) and the bis O-bonded $[Ru(bpy)_2(dmso)_2]^{2+}$ (dmso is dimethylsulfoxide; λ_{max} = 347, 496 nm; dmso solution) complexes both feature comparable absorption maxima.[34,61,62] This new complex is ascribed to O-bonded $[Ru(bpy)_2(OSO)]^+$ (hereafter, *O*-$[Ru(bpy)_2(OSO)]^+$). Comparison of these spectra indicates there is no apparent O-bonded complex present in solution with the S-bonded isomer.

The isomerization is reversible at room temperature in alcohol or propylene carbonate solution. In the absence of light, solutions of *O*-$[Ru(bpy)_2(OSO)]^+$ revert to *S*-$[Ru(bpy)_2(OSO)]^+$. Kinetic analysis reveals a biexponential decay with rate constants of 5.66(3) $\times$ 10^{-4} s^{-1} and 3.1(1) $\times$ 10^{-5} s^{-1}. While these rates are slower than those typically observed for O→S isomerization rates for monodentate dimethylsulfoxide,[30,31] they are in accord with rates for other chelating sulfoxide complexes.[16,29,37] The biexponential behavior demands explanation with just a single sulfoxide for isomerization. One interpretation is that

(59) Roeker, L.; Dobson, J. C.; Vining, W. J.; Meyer, T. J. *Inorg. Chem.* **1987**, *26*, 779–781.
(60) Root, M. J.; Deutsch, E. *Inorg. Chem.* **1985**, *24*, 1464–1471.
(61) Smith, M. K.; Gibson, J. A.; Young, C. G.; Broomhead, J. A.; Junk, P. C.; Keene, F. R. *Eur. J. Inorg. Chem.* **2000**, 1365–1370.
(62) Durham, B.; Wilson, S. R.; Hodgson, D. J.; Meyer, T. J. *J. Am. Chem. Soc.* **1980**, *102*, 600–607.

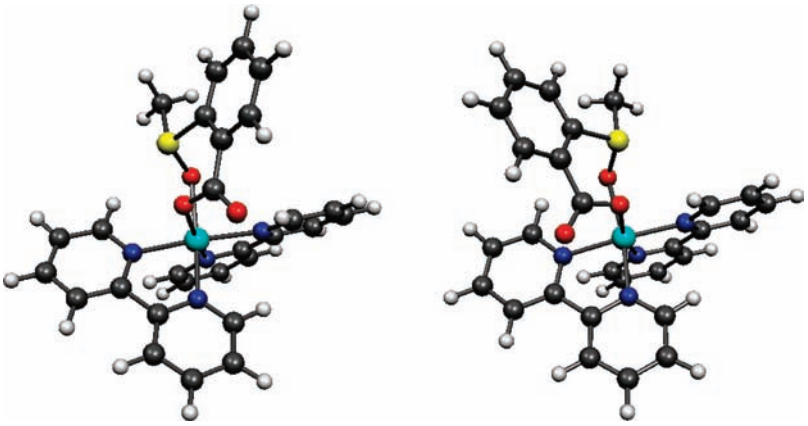

Figure 4. Structures of two O-bonded metastable states as calculated from DFT.

irradiation produces two O-bonded isomers that are spectroscopically and electronically similar. In that case, the two rates correspond to conversion of each O-bonded isomer to *S*-$[Ru(bpy)_2(OSO)]^+$ or conversion of one isomer to the second and then to *S*-$[Ru(bpy)_2(OSO)]^+$. The former case requires two distinct transition states, whereas the latter case requires one transition state for this isomerization.

On the basis of these O→S kinetic results, we questioned if two ground-state singlet O-bonded isomers were present in solution. There is clearly evidence for two such structures in the ^{1}H NMR spectrum, which features two sets of aromatic peaks and two resonances for the unique S-CH_3 group.[37] Accordingly, DFT calculations reveal two ground-state singlet O-bonded isomers that differ only in the orientation of the benzoic acid ring relative to the rest of the molecule. Shown in Figure 4 are these two structures viewed down the $Ru-O_{benzoate}$ bond. These two structures are related to one another through a simple reflection of this ring through the plane containing $O_{benzoate}$, Ru, and $O_{sulfoxide}$. It should be noted that the TD-DFT results for these two isomers both show intense peaks corresponding to the peaks observed experimentally, one with ^{1}MLCT peaks at 469 nm (f = 0.1013) and 355 nm (f = 0.0515) and the other with ^{1}MLCT peaks at 480 nm (f = 0.1264) and 352 (f = 0.0541). Thus, the biexponential reversion from O to S that is observed in the UV−visible data is consistent with the presence of two separate isomers in solution.

Cyclic voltammograms of *S*-$[Ru(bpy)_2(OSO)]^+$ are consistent with electron-transfer-triggered isomerization of the sulfoxide.[63−70] In Figure 5 are shown representative voltammograms obtained in propylene carbonate solution at a scan rate of 0.1 V s^{-1}. The first scan shows a one-electron oxidation near 1.0 V assigned to the $Ru^{3+/2+}$ S-bonded couple. Upon reversing the polarity and scanning to less-positive potentials, two separate reductive waves are observed. The more positive wave is ascribed to reduction of S-bonded Ru^{3+}, while the less positive wave is ascribed to a new ruthenium complex. Reversing the scan reveals the corresponding oxidative wave for this lower-energy couple.

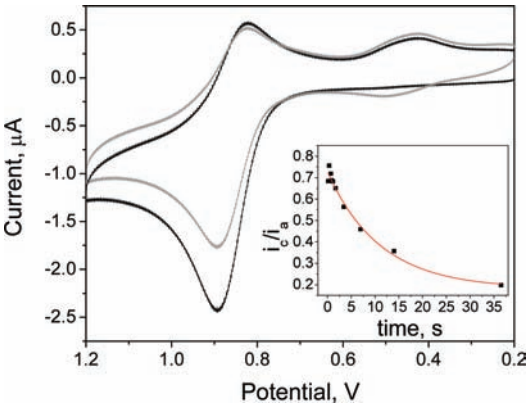

Figure 5. Cyclic voltammogram of *S*-$[Ru(bpy)_2(OSO)]^+$ in propylene carbonate. The first cycle (solid black line) shows only the S-bonded complex in solution, whereas the second cycle (gray line) shows evidence of both S- and O-bonded complexes in solution (ν = 0.1 V s^{-1}, glassy carbon working electrode, Pt counter electrode, Ag/Ag^+ reference electrode). Inset: plot of $(i_c)_o/(i_a)_o$ versus time fit to monoexponential decay (red line) to yield $k_{S\rightarrow O}$ on Ru^{III} formed from oxidation.

Current associated with the less positive couple is only observed following oxidation at 0.90 V, indicating that this species is only formed from the oxidation of S-bonded Ru^{2+}. As a result, this less positive couple is assigned to O-bonded $Ru^{3+/2+}$. Analysis of these voltammograms reveals $E_S^{\circ\prime}$ = 0.86 V and $E_O^{\circ\prime}$ = 0.49 V versus Ag/Ag^+ for the S- and O-bonded $Ru^{3+/2+}$ couples, respectively, in propylene carbonate. They are similar to the values observed in acetonitrile ($E_S^{\circ\prime}$ = 0.90 V and $E_O^{\circ\prime}$ = 0.54 V vs Ag/Ag^+). While $k_{O\rightarrow S}$ on Ru^{2+} can be directly measured from the O→S reversion formed from bulk photolysis (see above), $k_{S\rightarrow O}$ on Ru^{3+} may be extracted from voltammetric data collected at various scan rates. We determined $k_{S\rightarrow O}$ from the slope of a plot of $(i_c)_o/(i_a)_o$ versus time, where $(i_a)_o$ and $(i_c)_o$ are the anodic and cathodic peak currents for the $Ru_S^{3+/2+}$ couple.[39,71] In this plot, time is determined from the scan rate and the applied switching potential. By altering the time permitted for isomerization (variation in scan rate), differing concentrations of S- and O-bonded isomers are formed on the electrode. We found $k_{S\rightarrow O}$ = 0.090(15) s^{-1} in propylene carbonate and $k_{S\rightarrow O}$ = 0.11(3) s^{-1} in acetonitrile, which is considerably slower than has been reported for other sulfoxide isomerizations on ruthenium polypyridyl complexes following oxidation. For example, $k_{S\rightarrow O} \sim 50-100$ s^{-1} for complexes of the

(63) Nicholson, R. S.; Shain, I. *Anal. Chem.* **1964**, *36*, 706–723.
(64) Sano, M. *Struct. Bonding (Berlin)* **2001**, *99*, 117–139.
(65) Sano, M.; Taube, H. *Inorg. Chem.* **1994**, *33*, 705–709.
(66) Tomita, A.; Sano, M. *Inorg. Chem.* **1994**, *32*, 5825–30.
(67) Tomita, A.; Sano, M. *Inorg. Chem.* **2000**, *39*, 200–205.
(68) Yeh, A.; Scott, N.; Taube, H. *Inorg. Chem.* **1982**, *21*, 2542–2545.
(69) Johansson, O.; Lomoth, R. *Chem. Comm.* **2005**, 1578–1580.
(70) Johansson, O.; Lomoth, R. *Inorg. Chem.* **2008**, *47*, 5531–5533.
(71) Nicholson, R. S. *Anal. Chem.* **1966**, *38*, 1406–1406.

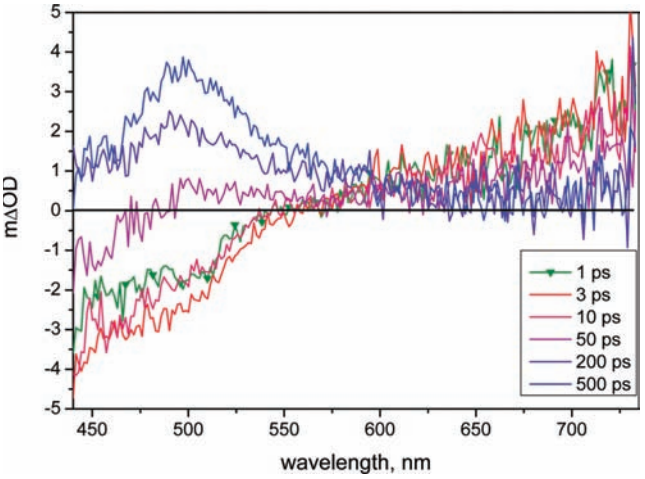

Figure 6. Picosecond transient absorption spectra of *S*-$[Ru(bpy)_2(OSO)]^+$ in methanol. Monoexponential fit (Supporting Information) of kinetic trace at 500 nm yields $\tau = 150$ ps.

type $[Ru(tpy)(L2)(dmso)]^{n+}$, where L2 is a variable bidentate ligand of neutral or anionic charge.[30,31,36] Apparently, the chelate effect in $[Ru(bpy)_2(OSO)]^+$ hinders S→O isomerization following oxidation of Ru^{2+}.

The photoisomerization quantum yield ($\Phi_{S\rightarrow O} = 0.45$, methanol) is quite large, indicating a rapid excited state isomerization rate constant.[33] The picosecond transient absorption spectra of *S*-$[Ru(bpy)_2(OSO)]^+$ in methanol are shown in Figure 6. In the first 3 ps following excitation at 400 nm, the bleach or negative peak from 440 to 550 nm grows in intensity. In accord with other ultrafast studies involving ruthenium polypyridine complexes, we attribute this to vibrational cooling of the ^{3}MLCT excited state, despite its relatively slow rate.[72−83] From ~3 to 500 ps, a steady increase in intensity of a peak near 500 nm is observed with the appearance of an isosbestic point near 600 nm. The kinetic trace at 500 nm is monoexponential with $\tau = 150$ ps (Supporting Information). The traces from 500 to 1500 ps (not shown for clarity) are essentially identical to the ground-state absorption spectrum of *O*-$[Ru(bpy)_2(OSO)]^+$, indicating that the O-bonded ground state is formed from excitation of *S*-$[Ru(bpy)_2(OSO)]^+$ on this time scale. Moreover, it appears that ground-state *O*-$[Ru(bpy)_2(OSO)]^+$ is formed *directly* from an S-bonded ^{3}MLCT state of $[Ru(bpy)_2(OSO)]^+$.

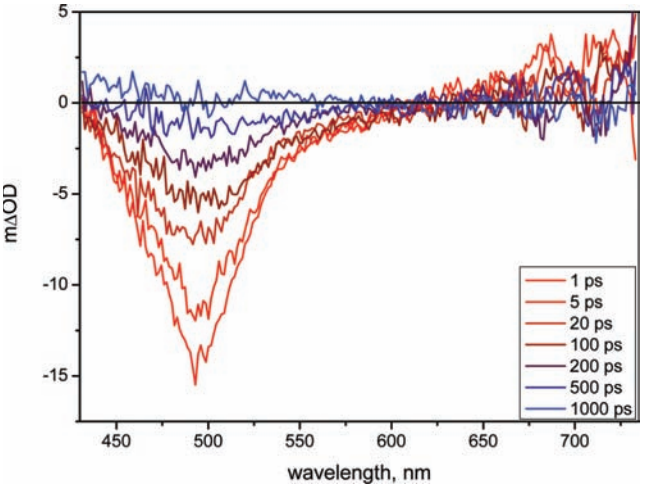

Figure 7. Picosecond transient absorption spectra of *O*-[Ru(bpy)2 $(OSO)]^+$ in methanol. Biexponential fit (Supporting Information) of kinetic trace at 496 nm yields $\tau_1 = 10$ ps and $\tau_2 = 205$ ps.

In Figure 7 are shown the picosecond transient absorption spectra of *O*-$[Ru(bpy)_2(OSO)]^+$. The first trace at 1 ps is typical of many ruthenium polypyridine excited states and represents the vibrationally relaxed ^{3}MLCT. From 1 to 1000 ps, the bleach peak at 500 nm yields a transient that is indistinguishable from the zero line background spectrum, or ground-state *O*-$[Ru(bpy)_2(OSO)]^+$. This decay is biexponential with $\tau_1 = 10$ ps and $\tau_2 = 200$ ps (Supporting Information). The longer time constant is consistent with decay times for other O-bonded sulfoxide complexes.[33] We are uncertain of the assignment of this shorter kinetic phase. It is tempting to ascribe this feature to some subtle molecular rearrangement of ^{3}MLCT *O*-$[Ru(bpy)_2(OSO)]^+$ prior to relaxation to ground state *O*-$[Ru(bpy)_2(OSO)]^+$, as suggested above from the DFT calculations of *O*-$[Ru(bpy)_2(OSO)]^+$.

Surprisingly, there is no spectroscopic or kinetic evidence for an O-bonded ^{3}MLCT excited state in the spectral evolution of ^{3}MLCT *S*-$[Ru(bpy)_2(OSO)]^+$ to ground-state *O*-[Ru $(bpy)_2(OSO)]^+$. This finding is in contrast to our previous picosecond transient absorption studies on photochromic ruthenium terpyridine sulfoxide complexes.[33] In those investigations, we found that S→O isomerization occurred *along* the ^{3}MLCT surface and did not involve any surface hopping. The kinetic data presented here strongly support a mechanism in which isomerization involves surface jumping from the triplet excited state to the singlet ground state on a picosecond time scale. In this case, the vibrationally relaxed ^{3}MLCT *S*-$[Ru(bpy)_2(OSO)]^+$ must have a molecular geometry quite different from the initially formed Franck−Condon states. An η^2-type structure or asymmetric η^2 bonding seems a reasonable proposal. While such bonding remains unknown to us with respect to sulfoxides, such bonding interactions have been observed for SO_2. Indeed, irradiation of single crystals of S-bonded $[Ru(NH_3)_4(H_2O)(SO_2)]^{2+}$ or $[Ru(NH_3)_4Cl(SO_2)]^+$ yields both η^2-SO_2 and O-bonded OSO metastable states at low temperatures.[84−86]

(72) Bhasikuttan, A. C.; Suzuki, M.; Nakashima, S.; Okada, T. *J. Am. Chem. Soc.* **2002**, *124*, 8398–8405.
(73) Curtright, A. E.; McCusker, J. K. *J. Phys. Chem. A* **1999**, *103*, 7032–7041.
(74) Damrauer, N. H.; Boussie, T. R.; Devenney, M.; McCusker, J. K. *J. Am. Chem. Soc.* **1997**, *119*, 8253–8268.
(75) Damrauer, N. H.; Cerullo, G.; Yeh, A.; Boussie, T. R.; Shank, C. V.; McCusker, J. K. *Science* **1997**, *275*, 54–87.
(76) Damrauer, N. H.; McCusker, J. K. *J. Phys. Chem. A* **1999**, *103*, 8440–8446.
(77) Damrauer, N. H.; McCusker, J. K. *Inorg. Chem.* **1999**, *38*, 4268–4277.
(78) Gawelda, W.; Johnson, M.; de Groot, F. M. F.; Abela, R.; Bressler, C.; Chergui, M. *J. Am. Chem. Soc.* **2006**, *128*, 5001–5009.
(79) McCusker, J. K. *Acc. Chem. Res.* **2003**, *36*, 876–887.
(80) McFarland, S. A.; Lee, F. s.; Cheng, K. A. W. Y.; Cozens, F. L.; Schepp, N. P. *J. Am. Chem. Soc.* **2005**, *127*, 7065–7070.
(81) Ramakrishna, G.; Jose, D. A.; Kumar, D. K.; Das, A.; Palit, D. K.; Ghosh, H. N. *J. Phys. Chem. B* **2006**, *110*, 10197–10203.
(82) Wallin, S.; Davidsson, J.; Modin, J.; Hammarstrom, L. *J. Phys. Chem. A* **2005**, *109*, 4697–4704.
(83) Yeh, A. T.; Shank, C. V.; McCusker, J. K. *Science* **2000**, *289*, 935–938.
(84) Bowes, K. F.; Cole, J. M.; Husheer, S. L. G.; Raithby, P. R.; Savarese, T. L.; Sparkes, H. A.; Teat, S. J.; Warren, J. E. *Chem. Comm.* **2006**, 2448–2450.
(85) Kovalevsky, A. Y.; Bagley, K. A.; Cole, J. M.; Coppens, P. *Inorg. Chem.* **2003**, *42*, 140–147.
(86) Kovalevsky, A. Y.; Bagley, K. A.; Coppens, P. *J. Am. Chem. Soc.* **2002**, *124*, 9241–9248.

At least for SO_2, the obvious transition state for isomerization from S-bonded to O-bonded can be stabilized and observed as an intermediate in these structures. Quantum chemical DFT calculations confirm the existence of metastable linkage isomers of SO_2 in these complexes.[87] Moreover, such seven-coordinate intermediates are actually stabilized in 17 e^- complexes or, by inference, excited state structures, according to certain ab initio calculations.[88,89]

Additional support for an η^2 or asymmetric η^2-bonding structure comes from the emission spectra. If the molecular structure of the thermally relaxed excited state complex is disparate from the ground state, then one expects a larger reorganization than is typically found for charge-transfer complexes of this type. Accordingly, the Stokes' shift ($E_{max,abs} - E_{max,em}$) for $[Ru(bpy)_2(OSO)]^+$ is ~8000 cm^{-1}, which is considerably larger than the Stokes' shift of ~5800 cm^{-1} for $[Ru(bpy)_3]^{2+}$. Assuming that the singlet−triplet MLCT energy gap is similar in both compounds (~3500−4000 cm^{-1}), then the additional energy can be assigned in part to a greater distortion (reorganization) in these complexes relative to $[Ru(bpy)_3]^{2+}$. Such a large distortion and rearrangement may explain the relatively slow IVR rate (~1−3 ps) in comparison to other ruthenium polypyridine complexes.

In aggregate, these data can be combined to yield a more complete picture of isomerization in photochromic ruthenium complexes containing a chelating sulfoxide (Figure 8). Excitation of *S*-$[Ru(bpy)_2(OSO)]^+$ promotes an electron from an orbital that contains ruthenium and significant sulfoxide character to an orbital that is located on a bipyridine. Similar to $\pi \rightarrow \pi^*$ excitations in stilbenes and other rhodopsin mimics,[90] this action permits rotation of the sulfoxide relative to the Ru−S bond and prompts movement of the sulfoxide during formation of the vibrationally relaxed ^{3}MLCT *S*-$[Ru(bpy)_2(OSO)]^+$. Also, this transition prompts shortening of the $Ru-O_{benzoate}$ bond (cis to the sulfoxide), a movement we have suggested is important in these excited-state isomerizations. DFT calculations support this interpretation, as MLCT oxidation will lengthen the Ru−S bond and shorten the $Ru-O_{benzoate}$ bond. Since the data do not support the formation of an O-bonded excited state, we propose that the minimum structure on the excited state surface corresponds to a maximum on the ground-state surface. An η^2-sulfoxide or asymmetric η^2-sulfoxide bonding model is proposed. Surface jumping is thus a nonadiabatic process occurring at a conical intersection with τ = 150 ps from the ^{3}MLCT surface to the singlet ground-state surface. The proposed conical intersection is formed from reaction coordinates involving sulfoxide rotation and Ru−S bond length changes.

In conclusion, we have found evidence for direct isomerization from an S-bonded excited state to an O-bonded ground state. In comparison to previous results regarding the isomerization characteristics of monodentate dimethylsufloxide bound to ruthenium(II), it is striking that the chelate results in a dramatic change in mechanism. Future investigations will involve time-resolved studies of similar complexes as well as the preparation of new complexes in order to better understand these changes in mechanism.

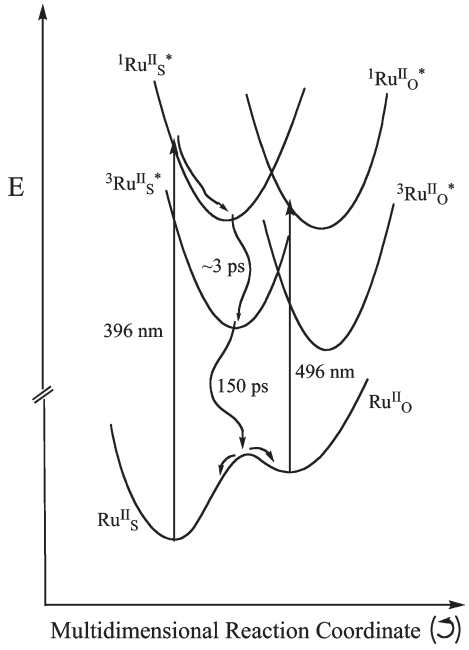

Figure 8. Proposed energy level diagram depicting isomerization as a nonadiabatic surface-jumping event. Ligand field surfaces are omitted for clarity.

Acknowledgment. We thank Michael P. Jensen, P. Greg Van Patten, and Hugh H. Richardson for helpful discussions in preparing this manuscript. We are grateful to Dr. E. O. Danilov for experimental assistance and OLKS at BGSU for access to the picosecond transient absorption spectrometer employed in these studies. J.J.R. thanks NSF (CHE 0809669), Ohio University, Condensed Matter and Surface Science (CMSS), NanoBioTechnology Initiative (NBTI), and the Nanoscale and Quantum Phenomena Institute (NQPI) for funding. B.A.M. recognizes NDSEG for a fellowship. C.T. thanks NSF (CHE 0503666) and the Ohio Supercomputer Center for their generous support. D.A.L. thanks OSU for a University Presidential Graduate Fellowship.

Supporting Information Available: Tables of DFT calculations of $[Ru(bpy)_2(OS)]^+$ and $[Ru(bpy)_2(OSO)]^+$ and related complexes, kinetic traces and fits from picosecond spectra, a CIF file for 2-methylsulfinylbenzoic acid ($C_8H_8SO_3$), and complete ref 43. This material is available free of charge via the Internet at http://pubs.acs.org.

(87) Marchenko, A. V.; Vedernikov, A. N.; Huffman, J. C.; Caulton, K. G. *New. J. Chem.* **2003**, *27*, 680–683.
(88) Lin, Z.; Hall, M. B. *J. Am. Chem. Soc.* **1992**, *114*, 6574–6575.
(89) Lin, Z.; Hall, M. B. *Inorg. Chem.* **1992**, *31*, 2791–2797.
(90) Waldeck, D. H. *Chem. Rev.* **1991**, *91*, 415–436.